MOLECULAR AND CELLULAR BIOLOGY
2023, VOL. 43, NO. 6, 241–253
https://doi.org/10.1080/10985549.2023.2198167

Taylor & Francis
Taylor & Francis Group

RESEARCH ARTICLE

Phosphorylation of the Myogenic Factor Myocyte Enhancer Factor-2 Impacts Myogenesis In Vivo

Kumar Vishal, Elizabeth Barajas Alonso, Ashley A. DeAguero, Jennifer A. Waters, Maria B. Chechenova, Richard M. Cripps

Department of Biology, San Diego State University, San Diego, California, USA

ABSTRACT Activity of the myogenic regulatory protein myocyte enhancer factor-2 (MEF2) is modulated by post-translational modification. We investigated the in vivo phosphorylation of *Drosophila* MEF2, and identified serine 98 (S98) as a phosphorylated residue. Phospho-mimetic (S98E) and phospho-null (S98A) isoforms of MEF2 did not differ from wild-type in their activity in vitro, so we used CRISPR/Cas9 to generate an S98A allele of the endogenous gene. In mutant larvae we observed phenotypes characteristic of reduced MEF2 function, including reduced body wall muscle size and reduced expression of myofibrillar protein genes; conversely,*S98A* homozygotes showed enhanced MEF2 function through muscle differentiation within the adult myoblasts associated with the wing imaginal disc. In adults, *S98A* homozygotes were viable with normal mobility, yet showed patterning defects in muscles that were enhanced when the *S98A* allele was combined with a *Mef2* null allele. Overall our data indicate that blocking MEF2 S98 phosphorylation in myoblasts enhances its myogenic capability, whereas blocking S98 phosphorylation in differentiating muscles attenuates MEF2 function. Our studies are among the first to assess the functional significance of MEF2 phosphorylation sites in the intact animal, and suggest that the same modification can have profoundly different effects upon MEF2 function depending upon the developmental context.

KEYWORDS MEF2, *Drosophila*, muscle, myoblast, transcription, phosphorylation

INTRODUCTION

Myocyte enhancer factor-2 is a member of the MADS (*MCM1*, agamous, deficiens, serum response factor) domain family of transcriptional regulators that play critical roles in a variety of developmental contexts (reviewed in Potthoff and Olson[1]). Prominent amongst these roles is the regulation of muscle differentiation, where MEF2 factors are known to bind to AT-rich sequences in the promoters of a large number of mammalian myofibrillar protein genes to enhance their expression.[2,3] This transcriptional function for MEF2 is highly conserved across the animal kingdom, with cognate MEF2 factors shown to regulate muscle gene expression in *Drosophila*.[4–6] Moreover, MEF2 factors are essential in vivo for downstream activation of the muscle regulatory program, since mutation of *mef2* genes results in defects in muscle formation. For example in mice, *mef2c* function is required early during development for heart and smooth muscle differentiation[5,7] and at birth for normal skeletal muscle maintenance.[8] *mef2a* null mutant mice die around birth due to cardiovascular defects.[9] In zebrafish, combined knockdown of *mef2c* and *mef2d* results in defects in muscle assembly.[10] Similarly, in *Drosophila* the single-copy *Mef2* gene is essential for differentiation of both embryonic and adult muscle lineages.[11–14]

Nevertheless, the regulation of MEF2 activity is complex. Given that MEF2 factors also contribute to the development of additional tissues, such as the immune system and nervous system (reviewed in Potthoff and Olson[1]) MEF2 function must be

Address correspondence to Richard M. Cripps rcripps@sdsu.edu.

The authors have no potential competing interests.

Received 2 June 2022
Revised 14 March 2023
Accepted 15 March 2023

interpreted in a cell-type specific context. This could occur via cell-specific post-transcriptional modification, or via interaction will tissue-specific co-factors, or a combination of these mechanisms. Indeed, numerous studies have investigated the impact of protein kinases upon MEF2 function, including analyzing effects of these modifications upon DNA binding in vitro and transactivation in tissue culture assays (reviewed in Black and Cripps[15]).

In addition, several reports have noted that MEF2 protein is detected in myoblasts significantly prior to the onset of muscle differentiation, which has raised the question as to how and why MEF2 activity may be restrained before cells receive a signal to differentiate. In the *Drosophila* embryo, for example, MEF2 is detected by stage 6 of embryonic development,[13] but the earliest detectable phenotypes are a loss of target gene expression at stage 11[16] and a failure of myoblast fusion at stages 13–14.[11,13] Similarly, the adult myoblasts associated with the larval imaginal discs show MEF2 accumulation at least 18 h prior to a demonstrated role in adult myogenesis.[12,14,17]

At least two mechanisms have been documented for the post-translational attenuation of MEF2 function. Several groups characterized a phosphorylation-dependent interaction of MEF2 with the class II histone deacetylases (HDACs) 4, 5 and 7, in which MEF2 bound to DNA and complexed with HDAC4 was unable to activate muscle differentiation. Phosphorylation of HDACs results in their nuclear exclusion and release of MEF2 to initiate muscle differentiation.[18–22]

In addition, post-translational modification of MEF2 has been associated with regulation of its function. Prominent among the modifications is phosphorylation, that has been shown to regulate DNA binding ability[23] and transactivation ability (see for example Han et al.[24] and Cox et al.[25]) Several cellular signaling pathways also converge upon MEF2 to trigger its modification and impact its activity (reviewed in Black and Cripps[15]) Importantly, p38 MAP kinase has been shown to directly modify several MEF2 residues in vitro in MEF2A,[25] and P38 action on MEF2 potentiates its activity in tissue culture studies.[26] Modification of MEF2 by p38 likely arises from a direct physical interaction between the two polypeptides, via a short p38 docking domain as defined in MEF2A.[26]

Phosphorylation of MEF2 does not just increase its activation function: Badodi et al.[27] recently noted that MEF2 levels in C2 cells fluctuate during the cell cycle, being significantly reduced in the G2 and S phases. The reduction in MEF2 levels during the cell cycle arises from phosphorylation of the conserved serine residues S98 and S110, which trigger degradation of MEF2 mediated by the ubiquitin ligase *SKP2*.[27,28]

These studies underline the importance of post-translational regulation of MEF2 function in the cell. Nevertheless, there is still much to learn of the in vivo modification of MEF2 in intact organisms, and of its functional significance during development. In this paper, we demonstrate that MEF2 is phosphorylated in vivo in *Drosophila* at S98, and we test the requirement for this modification by generating an unmodifiable *S98A* allele of the endogenous *Mef2* locus using CRISPR/Cas9 genome editing. Detailed phenotypic analyses of the $Mef2^{S98A}$ mutants, which are homozygous viable, indicated that the *S98A* allele causes a reduction in MEF2 function during muscle differentiation, but an increase in MEF2 function in myoblasts. These studies are among the first to define in vivo the significance of MEF2 post-translational modifications, and underline how a similar modification might have opposite effects upon protein function depending upon the cellular context or developmental stage.

RESULTS

Generation and expression of a tagged Mef2 allele. To generate an isoform of MEF2 that could be purified from in vivo sources, we used the approach of Kyriakis et al.[29] to create a TAP (tandem affinity purification)-tagged version of MEF2. The design added a streptavidin binding moiety, a tobacco etch virus (TEV) protease site, and two protein G domains, fused in-frame to the C-terminus of MEF2. This hybrid cDNA was under the control of the inducible UAS promoter (Fig. 1A). To determine if

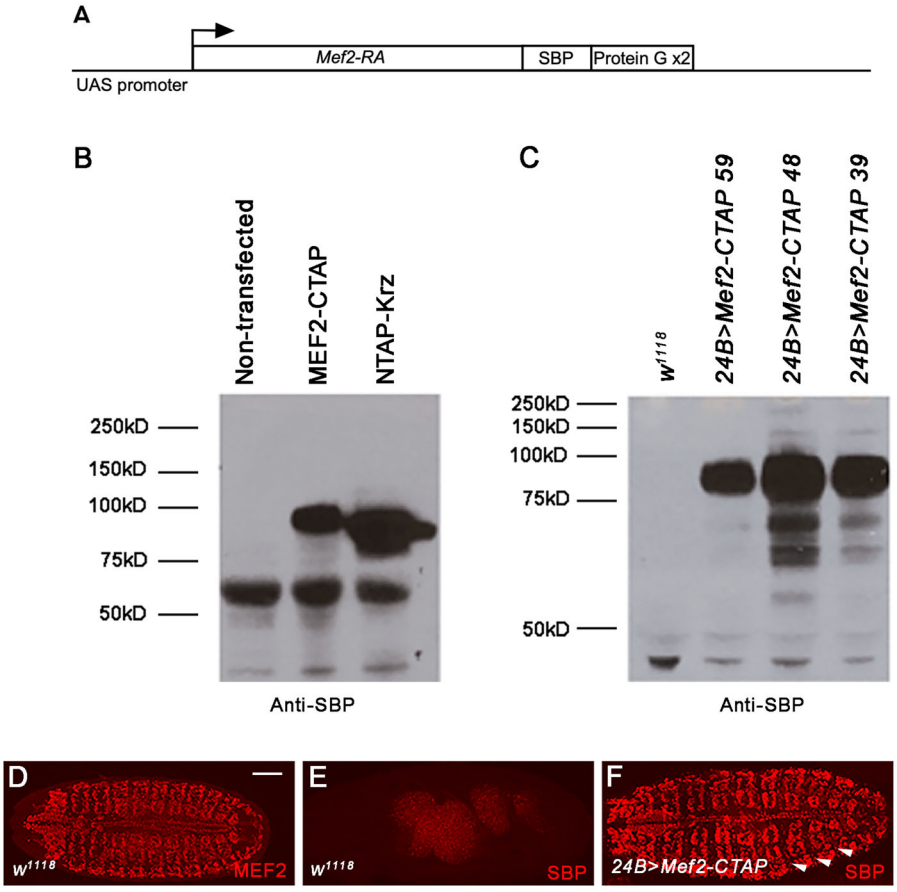

FIG 1 Generation and validation of UAS-Mef2-CTAP. (A) Diagram of construct generated for expression of C-terminally TAP-tagged *MEF2*. The inducible UAS promoter directs transcription of a fusion construct comprising the Mef2-RA cDNA, fused to streptavidin binding protein (SBP) and two protein G modules. Two tobacco etch virus (TEV) sites are located between the SBP and protein G regions (not shown). (B) Expression of TAP-tagged proteins was tested in *Drosophila* S2 tissue culture cells. Cells transfected with a constitutive Gal4 expression plasmid plus UAS plasmids expressing MEF2-CTAP or NTAP-Krz (lanes 2 and 3, respectively) showed accumulation of SBP-containing proteins of the correct predicted sizes. A smaller nonspecific band of apparent molecular mass 60 kD was detected in control plus experimental lanes. (C) Three independent transgenic lines carrying *UAS-Mef2-CTAP* were crossed to the mesodermal driver 24B-Gal4 and embryos aged 0–16 h were collected and processed for Western blotting with anti-SBP. Compared to control samples (lane 1), all three transgenic lines showed robust accumulation of MEF2-CTAP. (D to F) Embryos of the indicated genotypes were stained with either anti-MEF2 (D) or anti-SBP (E,F). (D) Control embryos show broad mesodermal accumulation of endogenous MEF2, with the punctate pattern indicating nuclear localization. (E) Control embryos do not accumulate proteins cross-reacting with anti-SBP. (F) *24B > Mef2-CTAP* embryos show broad mesodermal and nuclear accumulation of MEF2-CTAP. Arrowheads indicate accumulation of MEF2-CTAP in segment border cells. Bar for DF, 100 μm.

this construct directed the expression of full-length and tagged MEF2-CTAP, we transfected the cDNA into *Drosophila* S2 tissue culture cells alongside a plasmid constitutively expressing Gal4. Gal4 protein binds to the UAS sequence to activate expression of the fusion protein. As a positive control, we also expressed an N-terminally TAP-tagged isoform of the ß-arrestin Kurtz (Krz[29])

We used anti-SBP to detect expression of the fusion proteins. Although there was a background signal at 60 kD in both non-transfected and transfected cell lysates (Fig. 1B, lanes 1–3), the transfected cell lysates each showed accumulation of SBP-tagged protein at the expected apparent molecular weights (Fig. 1B, lanes 2–3). We concluded that the *Mef2-CTAP* construct could express full-length tagged MEF2 protein in a cellular system.

We next used P-element mediated germline transformation to generate transgenic lines carrying the *UAS-Mef2-CTAP* construct. Three independent lines were tested for their ability to express MEF2-CTAP by crossing transgenic flies to the mesodermal Gal4 line *24B-Gal4*.[30] From these crosses, embryos aged 0–16 h were harvested and assessed for transgene expression via Western blotting with anti-SBP. Non-transgenic w^{1118} embryos were used as a negative control. All three transgenic lines showed

robust accumulation of a ~90 kD polypeptide corresponding to CTAP-tagged MEF2 (Fig. 1C, lanes 2–4), whereas no signal at the same molecular mass was observed in the negative controls (lane 1).

To determine if the tagged MEF2 isoform accumulated in muscle nuclei in a manner similar to the localization of endogenous MEF2, we analyzed protein accumulation in fixed embryos at stage 16. At this stage, MEF2 in control w^{1118} embryos showed broad punctate accumulation in all muscle cells corresponding to the nuclear localization of this transcription factor (Fig. 1D). Whereas anti-SBP staining did not detect specific signal in control embryos (Fig. 1E), the SBP epitope was detected in *24B > Mef2-CTAP* embryos in a pattern highly similar to the accumulation of endogenous MEF2 (Fig. 1F). We observed additional MEF2-CTAP expression in cells at the segment border (Fig. 1F, arrowheads). These cells are likely to be tendon cells, since it has been documented that *24B-Gal4* is active in mesodermal cells plus tendon cells.[31]

Based upon these data, we concluded that we could successfully express TAP-tagged MEF2 in embryos, and that it stably accumulated in a nuclear pattern similar to endogenous MEF2.

Identification of S98 as a phosphorylated residue of MEF2 in vivo. To identify post-translational modifications of MEF2-CTAP, we used the affinity tags to attempt to purify MEF2-CTAP from *Drosophila* embryos. To achieve this, we crossed *24B-Gal4* adults to *UAS-Mef2-CTAP* en masse and collected approximately 5 g of embryos aged 0–16 h after egg laying. We also collected lysate from approximately 5 g of control w^{1118} embryos. We sought to purify MEF2-CTAP from embryo lysate based upon immobilizing the protein to IgG resin via the protein G tag and then eluting MEF2-SBP following TEV protease cleavage. While we were able to effectively cleave the protein G tag from MEF2-SBP, the protein remained lodged in the IgG column and could not be eluted. To address this complication, we instead purified MEF2-CTAP in a single step by binding to the IgG column, washing, and then eluting in SDS-PAGE sample buffer. When analyzed by SDS-PAGE and silver staining, we observed a ~90 kD band in the MEF2-CTAP lane that was absent in the control lane, albeit at low levels (Fig. 2A, arrow, compare lanes 1 and 2). We excised this band and submitted it for tandem mass spectrometry analysis. The analysis identified a limited number of MEF2 peptides that covered 64% of the MEF2-PA isoform that was expressed and purified (Fig. 2B). Importantly the spectrum covering serine-98 (S98) detected it as a phosphorylated residue, indicating that this amino acid is phosphorylated in vivo (Fig. 2C). Notably, this residue, and the surrounding amino acids, are strongly conserved across species (Fig. 2D), indicating that modification of this residue is likely to be an important control point for regulating MEF2 function.

Assessing the functional significance of MEF2 modification in tissue culture. To determine how $MEF2^{S98A}$ phosphorylation affects *Mef2* activity in vitro, we generated wild-type, $Mef2^{S98A}$, and $Mef2^{S98E}$ alleles of *Mef2* for expression in tissue culture cells, and assessed their ability to activate a MEF2-dependent reporter from the *ACTct57B* gene (*Act57B-lacZ*[4]). Wild-type MEF2 strongly activated the reporter compared to the empty expression vector, as did both $MEF2^{S98A}$ and $MEF2^{S98E}$ isoforms (Fig. 3A). We did not observe any significant difference in β-galactosidase activity between the wild-type and *Mef2* S98 alleles, each of which activated reporter expression to the same extent. These data indicated that any effect of S98 modification upon MEF2 function were too mild to be detected using these assays, and prompted us to determine if changes in MEF2 function through modification of S98 could be revealed using an in vivo system.

Generation of an S98A allele of Mef2 using CRISPR/Cas9 genome editing. To determine the functional significance of the S98 phosphorylation in vivo, we modified the endogenous *Mef2* gene by CRISPR/Cas9 genome editing, to generate a serine to alanine alteration (S98A). The overall design for this approach is shown in Fig. 3B, which depicts the relevant portion of the *Mef2* coding sequence and its corresponding predicted amino acid sequence. Part of the oligonucleotide sequence used for homology directed repair (HDR) is also indicated, with the red nucleotides corresponding

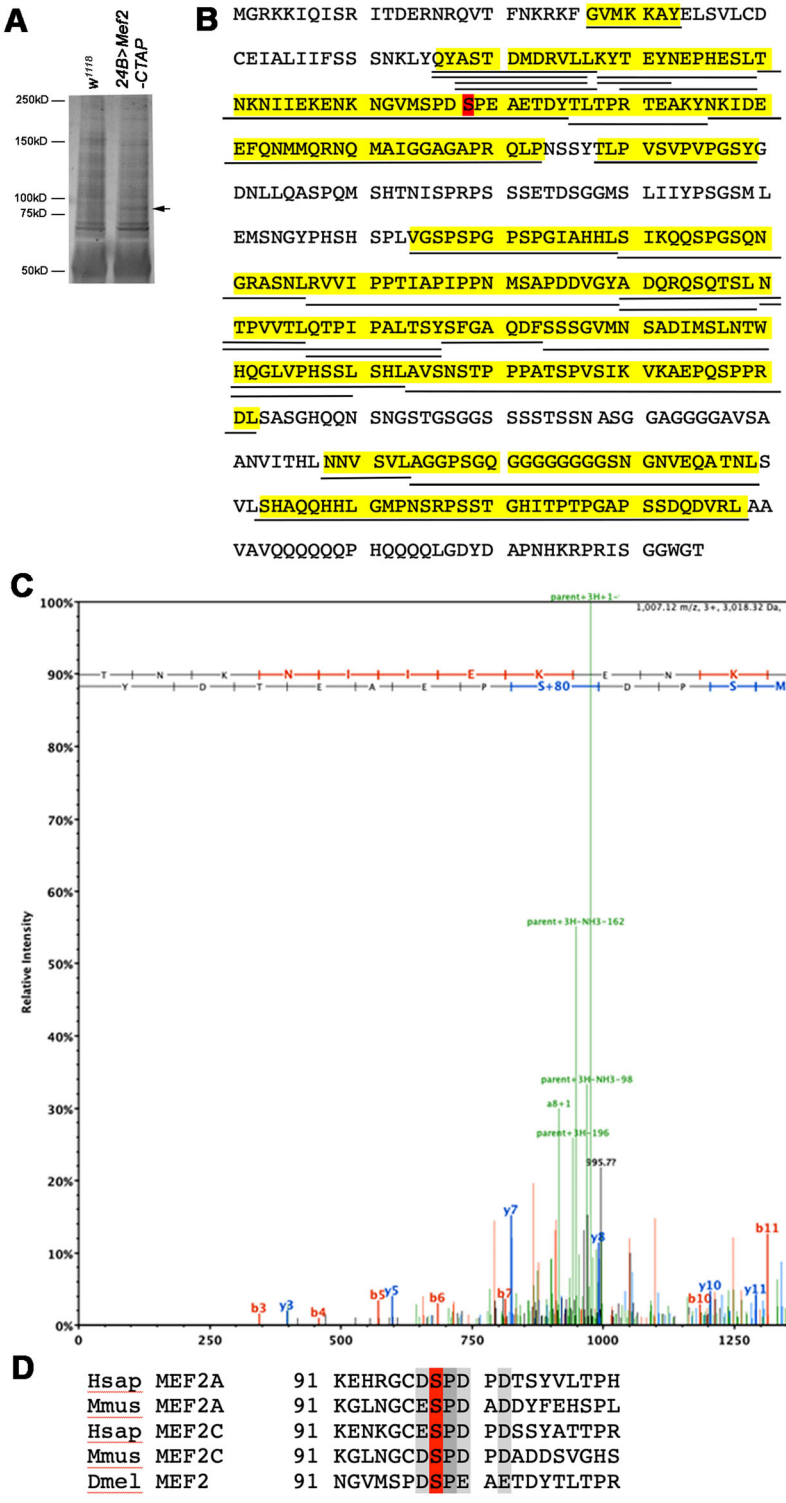

FIG 2 Purification and proteomic analysis of MEF2-CTAP. (A) Control embryos and embryos expressing *Mef2-CTAP* in the mesoderm were harvested, and TAP-tagged protein was purified using a single step purification (see text for details). Purified proteins were separated by SDS-PAGE and visualized by silver staining. A band corresponding to MEF2-CTAP was observed in the experimental lane but not the control lane. This band was excised and submitted for tandem mass spectrometry analysis. (B) Sequence of the MEF2-PA isoform, with yellow highlights indicate regions of the protein for which peptides were detected. The only phosphorylated residue was serine-98 (red highlight). (C) Mass spectrometry spectrum for the peptide containing phosphorylated Serine-98. (D) Sequence comparison between *Drosophila* MEF2 and human and murine MEF2A and MEF2C indicating that the serine-98 residue and immediately adjacent sequences are either identical or conserved in all five sequences.

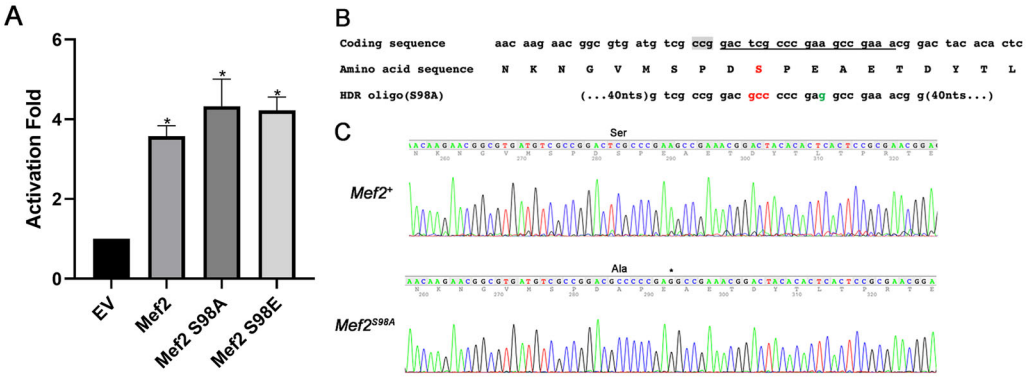

FIG 3 Activity of *MEF2* isoforms in tissue culture, and design and sequence analysis of the $Mef2^{S98A}$ allele. (A) Bar graph showing activation of the MEF2 target *Act57B-lacZ* by wild-type and mutant MEF2 isoforms in co-transfection assays. Note that all three MEF2 isoforms significantly activated reporter expression, but did not differ significantly from each other in the extent of that activation. (B) Top, coding sequence of *Mef2* surrounding serine-98. The protospacer and PAM (protospacer adjacent motif) are on the reverse strand, but their corresponding regions are shown as underline and grey highlight, respectively. Middle, amino acid sequence of the relevant region of MEF2, with S98 shown in red text. Bottom, partial sequence of the oligonucleotide used for homology directed repair (HDR) showing the intended edits in red (alteration of serine codon to alanine codon) and green (introduction of an *Ava*I restriction site that does not affect the coding sequence). (C) Sequence analysis of one confirmed $Mef2^{S98A}$ allele. Top, wild-type *Mef2* sequence with Ser codon indicated. Bottom, $Mef2^{S98A}$ allele showing the introduced Ala codon and the single nucleotide change to create the *Ava*I site (asterisk).

to an alanine codon. We also included in the HDR sequence a silent mutation in codon E100, that would introduce an *Ava*I restriction site (5′-CYCGRG) to assist in diagnosing the modified locus following PCR amplification (green letter in HDR sequence). In the end, since the $Mef2^{S98A}$ allele proved to be homozygous viable, we did not use the restriction enzyme approach and simply direct-sequenced PCR products from candidate lines. Using this approach, we isolated two lines in which the correct edits had been generated in *Mef2* with no other mutations to the coding sequence detected (Fig. 3C). The $Mef2^{S98A}$ mutant allele retained significant MEF2 function since the flies were viable and fertile as homozygotes. Note that the two lines derived from independent G0 founder adults, indicating that they arose from independent editing events. In the phenotypic analyses below, we demonstrate that both lines share the most significant phenotypic effects, and distinguish the alleles by designating them S98A-1 and S98A-2.

Phenotypic analysis of $Mef2^{S98A}$ larvae. While the $Mef2^{S98A}$ homozygotes were viable, we nevertheless reasoned that there might be subtle effects of this mutation upon MEF2 function and thereby muscle formation. To test this hypothesis, we first examined whether this mutation in *Mef2* gene affects third instar wing disc associated myoblast differentiation. Normally, these myoblasts remain in an undifferentiated proliferative state throughout the three larval instars, and then undergo differentiation during the early pupal stage to form the adult muscles. While we did not see any signs of muscle differentiation in the wild-type wing disc myoblasts ($n = 23$ discs stained for F-actin and MHC accumulation), a portion of the $Mef2^{S98A}$ homozygotes exhibited muscle specific protein expression in the myoblasts. F-actin was detected in the wing disc of 13.6% of the $Mef2^{S98A\text{-}1}$ mutants ($n = 22$) and 16.7% of the $Mef2^{S98A\text{-}2}$ mutants ($n = 24$). MHC accumulation was observed in 11.1% and 12.5% of the $Mef2^{S98A\text{-}1}$ ($n = 27$) and $Mef2^{S98A\text{-}2}$ ($n = 22$) mutants, respectively (Fig. 4A to F). Thus, our results demonstrate that $Mef2^{S98A}$ homozygotes prematurely activate muscle differentiation in the wing disc myoblasts. This phenotype was reminiscent of the effect of overexpression of *Mef2*, which also resulted in activation of myogenic program in the wing disc associated myoblasts.[32] Since premature muscle differentiation of myoblasts might attenuate proliferation and deplete their pool size, we also compared the total number of wing disc associated myoblasts in the wild-type and $Mef2^{S98A\text{-}1}$ homozygotes. However we did not observe any significant difference in the number of wing disc myoblasts between control and experimental flies (Fig. 4G to I). Taken together, our results suggest that the $Mef2^{S98A}$ mutation moderately increased MEF2 function in the myoblasts.

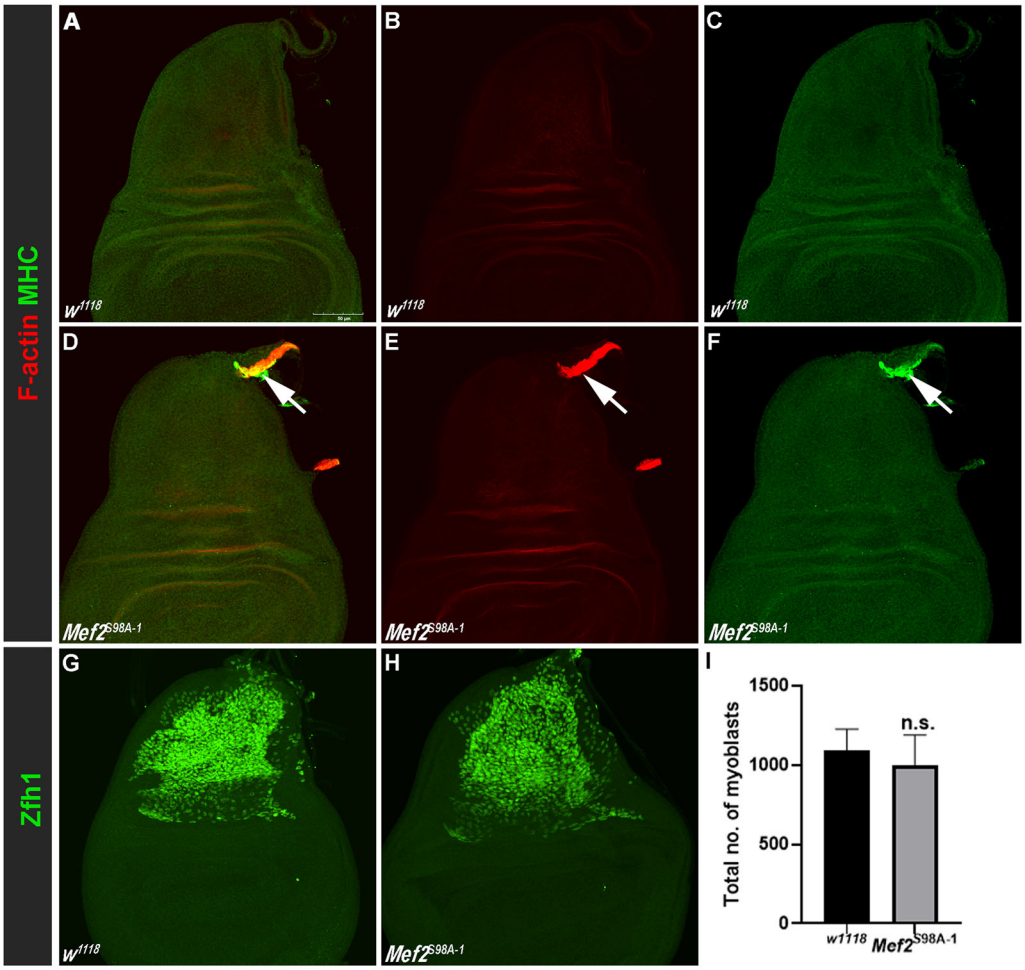

FIG 4 Premature differentiation in wing imaginal discs. (A to F) Confocal micrographs of wandering third instar wing imaginal discs double-labelled for MHC (green) and F-actin (red).There is a complete absence of MHC and F-actin staining in wild-type discs (A to C). (D to F) *Mef2*$^{S98A-1}$ discs show both MHC and F-actin staining. (G to H) Wild-type and *Mef2*$^{S98A-1}$ discs associated myoblasts stained with ant-Zfh1 antibody. (I) Bar graph showing no significant difference between wild-type and mutant myoblast pool. Scale bar, 50 μm.

Since MEF2 contributes to multiple myogenic events, we next examined the effect of the *Mef2*^{S98A} mutation on the larval body wall muscles. We focused our analyses on one of the largest body wall muscles, VL3, where we compared VL3 muscle area and the number of myonuclei between wild-type and *Mef2*^{S98A} mutants in wandering third instar larvae. We found that the area occupied by VL3 muscles in both mutants was significantly lower than in the wild-type samples (Fig. 5A to C). This reduction in the muscle area in mutants might be either due to reduced muscle differentiation or due to lower myoblast fusion resulting in fewer myonuclei. We did not observe any significant difference in the number of VL3 myonuclei between the wild-type and *Mef2*^{S98A} mutants, although we did note that the mutant nuclei appeared smaller than control nuclei (Fig. 5D). Thus, our data demonstrated that the thinner VL3 muscle in *Mef2*^{S98A} samples was not due to lack of myoblast fusion or loss of myonuclei, but instead may arise from impaired muscle growth.

To further understand how blocking MEF2 S98 phosphorylation resulted in a reduced MEF2 function during larval body wall muscle growth, we compared the expression levels of three known MEF2 target genes, *Troponin I* (*TnI*, also called *wings-up A*), *Myosin heavy chain* (*Mhc*) and *Actin 57B* (*Act57B*) between the wild-type and mutant flies. There were significant reductions in *TnI* and *Act57B* transcript levels in *Mef2*$^{S98A-1}$ mutants compared to controls, although *Mhc* transcript levels were not significantly reduced in the mutant (Fig. 5E). Our data suggest that S98A substitution

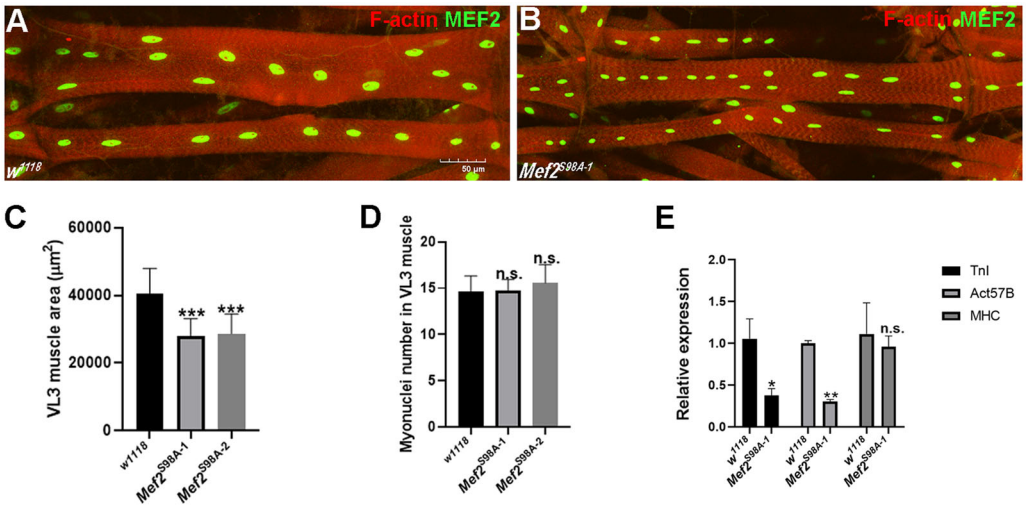

FIG 5 Reduced size of larval muscles. (A and B) Confocal microscope images of wild-type and mutant larval body wall muscles (VL3) double-stained for F-actin (red) and MEF2 (green). Scale bar for both panels, 50 µm. (C) Bar graph showing significant reduction in larval muscle area in mutant sample as compared to the control. (D) There was no significant difference in the number of myonuclei between wild-type and mutant muscles. (E) Bar graph showing significantly reduced *TnI* and *Act57B* expression in mutant larvae as compared to control samples. $^{*}p\leq0.05$; $^{**}p\leq0.01$; $^{***}p\leq0.001$.

impairs the ability of *MEF2* to activate the expression of at least a subset of muscle structural genes, which in turn results in thinner larval muscle fibers. Collectively, blocking MEF2^{S98} phosphorylation resulted in a phenotype characteristic of reduced MEF2 function during larval body wall muscle growth.

Phenotypic analysis of Mef2^{S98A} adults. To understand the impact of the *Mef2^{S98A}* mutation upon the mature adult muscle fibers, we analyzed the adult thoracic muscles. The indirect flight muscles (IFMs) consist of two muscle groups: the dorsal longitudinal muscles (DLMs) and dorsoventral muscles (DVMs). We analyzed stained cryosections to compare the number of DLM and DVM fibers between the control and experimental specimens. Our results showed that there were no significant differences in the number of DVM nor DLM fibers in control and experimental flies (Fig. 6A to D). We also flight-tested control and *Mef2^{S98A-1}* flies, but did not observe a loss of flight ability in the mutants (Fig. 6E). Overall, our results show that the *Mef2^{S98A}* mutation does not seriously affect IFM patterning nor differentiation.

However, we did observe defects in another adult muscle, the tergal depressor of the trochanter (TDT), or jump muscle, in the mutant flies. The wild-type jump muscle consists of approximately four small fibers at the anterior end of the muscles (labeled S in Fig. 6F), and 18–26 oblong-shaped large fibers. The large fibers are arranged in a distinct pattern, where each fiber has a surface that contacts both the outer and inner sides of the muscle[33] (Fig. 6F). Mutant flies homozygous for either the *S98A-1* or the *S98A-2* allele showed mis-aligned jump muscle fibers in approximately 60% of the cases: in these abnormal muscles, individual mutant fibers appeared pushed towards or away from the central region of the TDT, such that the affected fibers contacted only one surface of the muscle (asterisks in Fig. 6G). Similar abnormal patterning of the jump muscles has been observed when *Mef2* function is attenuated,[32,34] and we also observed this defect in homozygous escapers for *Mef2$^{44-5}$* (Fig. 6H), which is an hypomorphic *Mef2* allele.[35] Overall, these data suggest that the *S98A* allele attenuates MEF2 function in the context of TDT patterning.

In contrast, since adult myoblasts in the wing imaginal discs showed evidence of gain of MEF2 function, we also considered that defects in TDT patterning might also arise from gain of MEF2 function. To test this possibility, we assessed muscle formation in pharate adults in which *Mef2* was over-expressed using the *1151-Gal4* adult myoblast driver. Interestingly, these animals also showed defects in jump muscle patterning similar to those also observed for hypomorphic *Mef2* mutants (Fig. 6I). These observations indicated that both gain and loss of MEF2 function can impact

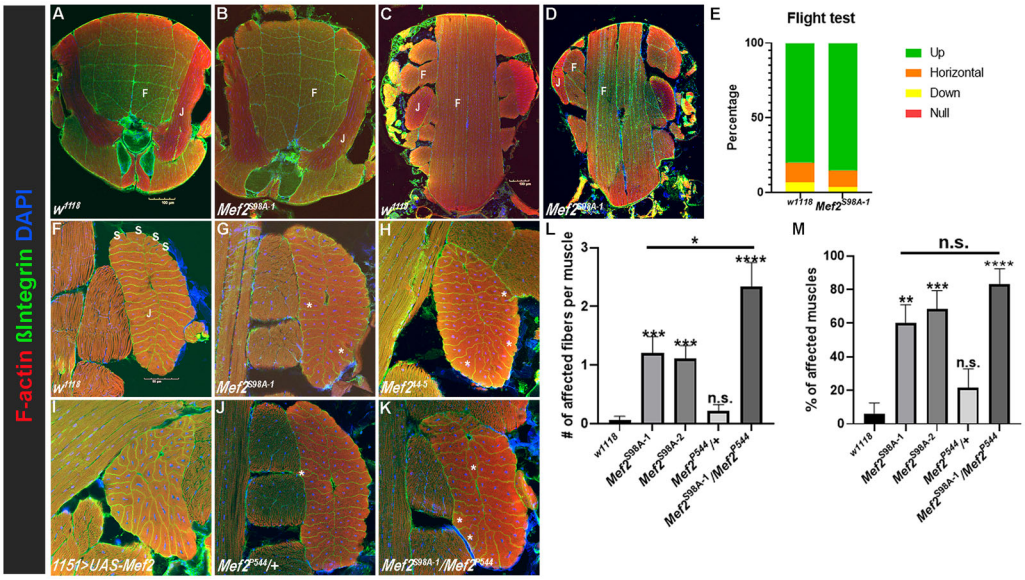

FIG 6 Effects of S98A substitution upon adult muscle function and patterning. (A and B) Transverse section of adult thoraces showing no difference in the number of DLM fibers in control (A) and mutant flies (B). Dorsal is to the top of the image. (C and D) Confocal images of horizontal section of adult thoraces showing no significant difference in the number of DVM fibers between the control and experimental flies. Anterior is to the top of the image. For A to D, F indicates flight muscle and J indicates jump muscle. (E) Bar graph showing no significant difference in the flight ability of control and $Mef2^{S98A-1}$ mutants. (F to K) Transverse section of jump muscles of wild-type (F), $Mef2^{S98A-1}$ (G) *1151>* *UAS-Mef2* (H), $Mef2^{44-5}$ (I), $Mef2^{P544/+}$ (J), $Mef2^{S98A-1/P544}$ (K). Anterior is to the top; small jump muscle cells are indicated with an S. (L) Bar graph showing significant patterning defects in $Mef2^{S98A}$ mutants and $Mef2^{S98A-1}/Mef2^{P544}$ compared to controls. (M) There is a significant increase in the number of samples showing patterning defects in mutant flies compared to wild-type. Scale bar: 100 μm for A to D, 50 μm for F to K.

organization of the jump muscle fibers, and that a critical balance of MEF2 function is necessary for normal jump muscle patterning.

To resolve whether the $Mef2^{S98A}$ jump muscle patterning phenotype arises from gain or loss of *MEF2* function, we combined the $Mef2^{S98A-1}$ allele with the $Mef2^{P544}$ null allele to generate $Mef2^{S98A-1}/Mef2^{P544}$ trans-heterozygotes. In these flies, we found that there was a significant increase in the number and frequency of defective fibers compared to control (Fig. 6J to M), demonstrating that the $Mef2^{S98A}$ mutation results in the attenuation of MEF2 function during patterning of the adult jump muscle.

DISCUSSION

In this manuscript we identified an in vivo phosphorylation site for the myogenic regulator MEF2, and assessed the in vivo requirement for phosphorylation of this residue through manipulation of the endogenous gene. To our knowledge, this is the first attempt to assess the functional significance of MEF2 phosphorylation in an intact animal through engineering of the endogenous locus. We note two main observations: firstly that blocking this modification of MEF2 resulted in relatively mild effects upon muscle formation; and secondly that modification of S98 appeared to have different effects upon MEF2 function depending upon the cellular context. The S98 codon, while lying outside of the highly conserved MADS/MEF2 domain, is nevertheless strongly conserved with mammalian MEF2 proteins, indicating that these findings in *Drosophila* are likely to be highly relevant to understanding vertebrate MEF2 function.

The relatively mild effects of the S98A substitution are in line with some prior observations assessing post-translational modification in vivo, where in many cases individual phosphorylation events fine-tune protein function, and only have a major impact when combined with modification of additional residues. For example, Kocherlakota et al.[36] assessed the roles of phosphorylated Tyr residues in the transmembrane protein sticks-and-stones (SNS) that is required for myoblast fusion. Only when 14 Tyr residues were altered to Phe was there a strong abrogation of SNS function, indicating that each individual modification may only have modest additive effects. In addition,

studies[27,28] have demonstrated that phosphorylation of MEF2 at S98 was generally accompanied by phosphorylation at S110, suggesting that a more profound impact upon MEF2 function might be achieved by generating an allele in which both residues were changed to alanine. Nevertheless, we also acknowledge that single phosphorylation events can have profound impacts upon protein function, including for *Drosophila* MEF2: phosphorylation of Tyr20 switches the function of MEF2 in the adult fat body from promoting expression of genes associated with anabolism to activating genes that function in the immune response.[37]

The observation of apparently opposite effects upon MEF2 function in different tissues resulting from the S98A substitution are noteworthy. We interpret the reduction in larval muscle mass and defects in jump muscle pattering to arise from loss of MEF2 function, and this conclusion is supported by the exacerbation of the latter phenotype when $Mef2^{S98A}$ is placed in trans to a *Mef2* null allele (this study). Moreover, hypomorphic mutations of *Mef2* are known to result in reductions in the level of expression of muscle structural protein genes,[38] and reduced expression of these structural genes would certainly account for the reduced muscle size that we observed. We also explored mechanisms through which gain of MEF2 function would result in smaller muscles. This might occur if, for example, myoblasts prematurely exited the cell cycle to form muscles prior to the generation of a normal myoblast pool, something that we observe at low, albeit nonsignificant, levels in the wing disc-associated myoblasts. In this scenario, the resulting muscles may grow more slowly through having fewer myonuclei. This latter possibility seems less likely, however, given both that the number of myonuclei does not differ significantly in mutant larvae compared to controls, and the number of disc-associated myoblasts exhibiting premature differentiation is small. We therefore conclude that these findings arise from a reduction of MEF2 function in the S98A isoform.

Gain of MEF2 function in myoblasts, resulting in premature differentiation in imaginal discs, is consistent with the demonstration that phosphorylation of MEF2 at S98 suppresses its myogenic activity, either through turnover via interaction with the ubiquitin ligase adaptor SKP2,[28] or through suppression of myogenic function through interaction with the prolyl isomerase PIN1.[39] While these pathways have not been demonstrated for *Drosophila* MEF2, one can hypothesize that the S98A form of MEF2 would be more stable and could promote myoblast differentiation. Although we have not tested the stability of the different MEF2 isoforms, the fact that each of them equivalently activate transcription in tissue culture, and the fact that the $Mef2^{S98A}$ alleles do not differ markedly from wild-type, suggests that there might not be major differences in their stability in tissue culture or in vivo.

To reconcile the apparently opposite effects upon MEF2 function of the S98A modification, we proposed the following hypothesis. The most reasonable solution is that the modification impacts MEF2 interaction with cofactors or other modulatory proteins, and that the identify of these proteins differs depending upon the developmental stage or cellular context. Numerous MEF2 co-factors have been identified, that either enhance or suppress activation of target genes. These include negatively acting factors such as those described above, plus class II HDACs discussed in the Introduction, MITR[18,40] and CABIN;[41] and positively acting cofactors such as MyoD in mammalian cells[42] and CF2 in *Drosophila*.[43] Future studies will be focused upon identifying how this post-translational modification can impact MEF2 function.

We also note that, since *Drosophila* MEF2 acts in tissues outside of the musculature,[1] the *S98A* mutation may impact those tissues to a greater extent than developing muscles. While this is a reasonable possibility, the animals used for proteomic analysis were at the embryonic stage, where MEF2 accumulation is overwhelmingly constrained to the mesoderm and muscular derivatives,[11,13] therefore we believe that the S98 phosphorylation is germane to muscle development.

Our future work will be aimed at identifying signaling pathways and downstream kinases that act on MEF2 S98 to regulate muscle growth and differentiation.

Furthermore, we plan to examine how other *Mef2 S98* substitutions affect MEF2 function.

MATERIALS AND METHODS

DNA methods. To generate the *Mef2-CTAP* allele, the *Mef2-RA* cDNA was amplified using PCR and cloned into pGEM-T Easy (Promega Corp) for subsequent cloning. The cDNA was excised from this plasmid and cloned into pUAST-CTAP(SG),[29] and in-frame fusion to the CTAP coding sequence was verified by sequencing.

The wild-type *pPAc-Mef2* expression plasmid was described in Kelly Tanaka et al.[43] Mutant variants were generated using the Q5 Site-directed Mutagenesis Kit (NEB), and validated by sequencing.

Quantitative PCR. RNA was isolated from a pool of 10 muscle carcasses each for wild-type and mutant flies using the miRNeasy Kit (Qiagen), according to the manufacturer's instruction. Three separate pools were used for the experiment. This was followed by synthesis of single strand complementary DNA (cDNA), generated from 100 ng of RNA using the iScript Advanced cDNA synthesis kit (Bio Rad). For quantitative PCR, cDNA samples were diluted 1:50 and mixed with SYBR Green Master mix (Bio-Rad) and appropriate primers.[43]

Fly stocks and genetics. Drosophila stocks used in this study were obtained from the Bloomington Drosophila Stock Center (BDSC), generated in the laboratory, or gifts from other groups. The *1151-Gal4* line was a gift from Dr. L. S. Shashidhara. *UAS-Mef2-CTAP* lines were generated by P-element mediated germline transformation,[44] and at least three independent lines were generated and validated.

To generate the $Mef2^{S98A}$ allele, a single guide RNA (sgRNA) targeting the *MEF2* gene close to the intended edit was ordered from IDT (protospacer sequence: 5′-TTTCGGCTTCGGGCGAGTC), as well as an sgRNA targeting the *ebony* gene as a co-CRISPR marker.[45] We used a 109-nt ssDNA oligonucleotide as a donor for homology directed repair, also from IDT. These reagents were injected into y vas-Cas9 embryos (BDSC) and surviving G0 adults were crossed to $CyRoi/Mef2^{44\text{-}5}$; *TM2/TM6* adults. Potential edited lines were identified in the G1 generation as adults showing the dark ebony body color, having received one recessive ebony allele from either of the *TM2* or *TM6* balancer chromosomes plus a CRISPR-generated ebony allele from the G0 parent. From approximately 40 G0 adults, of which 22 were fertile, eight independent G0 founders gave rise to offspring carrying a mutant ebony allele. Ebony G1 flies were crossed to a second chromosome balancer stock to generate stable lines, and candidate homozygous mutants were analyzed by PCR and direct sequencing using the forward and reverse oligonucleotides 5′-GAGGAGATGGTGAAATGTCGCC and 5′TTGGTGTGGGACATCTGTGG, respectively. Two independent lines arising from different G0 adults were isolated and used for analysis in this work.

Tissue culture and western blotting. For testing expression of TAP-tagged MEF2, tissue culture assays were performed using *Drosophila* S2 cells (*Drosophila* Genomics Resource Center) which were either nontransfected, transfected with pPAc-Gal4 plus UAS-Mef2-CTAP, or transfected with pPAc-Gal4 plus UAS-NTAP-Krz[29] using Lipofectamine (Thermo Fisher). Two days after transfection, cells were harvested and boiled in SDS-PAGE sample buffer. Western blotting was carried out using standard approaches and HRP-conjugated secondary antibodies.

For co-transfection assays, S2 cells were cultured in Schneider's medium at 25 °C and supplemented with 10% fetal bovine serum and 1% penicillin-streptomycin (Gibco). S2 cells were seeded at a concentration of 6×10^5 cells/well on a 24-well plate and allowed to adhere for an hour. After, the medium was removed and 300 μL of medium (serum and antibiotic free) that contained 0.5 μg of total plasmid DNA and 5 μL transfection reagent (FuGENE HD, Promega) was added to each well. Incubation was allowed for 24–32 h. The ratio of transcription factor coding pDNA (pPac-Pl) to reporter coding pDNA (*Act57B-lacZ*) was 1:9 (wt/wt). The same ratio was used for pPac-Pl vector controls that lacked the cDNA insert. Transient transfections were conducted in triplicate.

ß-Galactosidase assays. A mammalian β-galactosidase assay kit was used to lyse and determine the ß-galactosidase activity in the transfected cells (Pierce Technology, Thermo Scientific). To lyse cells, 100 μL of M-PER extraction reagent was added to each well, and incubated for 15 min while rotating at 350 rpm. The protein concentration of each lysate was determined by Bradford assay (Quick Start™ Bradford 1× Dye Reagent, Bio-Rad). Equal amounts of total lysate protein were used in ß-galactosidase assays, by using the appropriate volume of each lysate and making up to a standard volume by addition of extraction reagent. Next, equal volumes of cell lysate (plus extraction reagent) and all-in-one ß-galactosidase assay reagent were mixed in a 96-well plate and incubated at 37 °C for 30–45 min. After incubation, absorbances were read on a multiplate reader at 405 nm. Activation of the reporter was determined as the fold change of ß-galactosidase activity in samples cotransfected with TF DNA compared to controls cotransfected with the empty pPac-Pl vector.

Immunofluorescence and confocal microscopy. Wandering third instar larvae were dissected in PBS to obtain wing disc and muscle fillets, followed by fixation in 4% formaldehyde and immunolabeling as described by Vishal et al.[46] Adult flies were processed, cryosectioned and immunostained as described by Morriss et al.[47] Myoblast differentiation in imaginal discs was monitored using mouse anti-MHC (1:200, DSHB) and Alexa 568-conjugated Phalloidin (1:500, Thermo Fisher). Total myoblast numbers in discs were determined using rabbit anti-Zfh1 antibody (1:2000, Ruth Lehman). Larval body wall muscles and myonuclei were visualized as described in Morriss et al.,[47] using Alexa 568-conjugated Phalloidin and rabbit anti-MEF2 (1:1000),[46] respectively. Adult muscles were visualized using mouse anti-β-integrin (1:20, DSHB), Alexa 568-conjugated Phalloidin and DAPI. Alexa 488-conjugated secondary antibodies (Thermo Fisher) were used at 1:2000. The processed preparations were mounted on glass

slides using mounting solution and imaged with an Olympus FV 3000 confocal microscope. Images were processed using Olympus Life Science software and Adobe Photoshop CC 2018.

Quantification and data analysis. Myoblast differentiation was determined by counting the number of wandering third instar wing discs which were co-labelled with anti-MHC and F-actin; at least 18 discs were imaged for each genotype. Myoblast pools were analyzed by counting the total number of Zfh1-positive myoblasts in the late third instar wing discs of at least 11 discs. Wandering third larvae were used to compare muscle area between the control and mutant flies. Larval muscle area was determined using standard Image J measurement tool of the VL3 muscle from at least seven different animals. Larval myonuclei number was quantified by counting the total number of MEF2 positive nuclei of VL3 muscle of the A2 or A3 abdominal segments. Adult muscle patterning was examined by comparing the β-integrin positive muscle fascicles between the wild-type and experimental specimens and documenting the frequency and nature of the defects. Flight testing was carried out according to Drummond et al.,[48] using at least 50 adult females.

All quantifications were done using Image J software, and the data were imported into GraphPad Prism 6.0 software for the generation of graphs and statistical analyses. The statistical significance was determined using the column statistics function. Error bars represent the mean ± standard deviation for larval phenotypes, and the mean ± standard error of mean for adult phenotypes. Statistical significances were determined using one-way ANOVA plus post hoc tests for co-transfections, Student's *t* tests were used for myoblast counts and qPCR data, and Mann–Whitney tests were used for larval muscle measurements and analyses of adult jump muscles. The *n* represents the total number of samples quantified from two or more independent experiments.

ACKNOWLEDGEMENTS

We thank Dr A Veraksa for providing pUAST-CTAP(SG) and UAS-NTAP-Krz, and Dr Ruth Lehman for sharing rabbit anti-ZFh1 antibody. We acknowledge technical support from the Molecular Biology Facility.

FUNDING

This work was supported by R01 (GM124498) awarded by the NIH to RMC. AAD was supported by NIH grants R25 GM075149 and R25 HG007630. We acknowledge the Cell Biology Facility at the Department of Biology, University of New Mexico, supported by NIH grant P20 (GM103452) from the Institute Development Award (IdeA) Program of NIGMS.

DATA AVAILABILITY STATEMENT

The authors confirm that the data supporting the findings of this study are available at: https://figshare.com/articles/figure/Supporting_data_for_Vishal_et_al_2023/22294432

REFERENCES

1. Potthoff MJ, Olson EN. MEF2: a central regulator of diverse developmental programs. Development. 2007;134:4131–4140. doi:10.1242/dev.008367.
2. Andres V, Cervera M, Mahdavi V. Determination of the consensus binding site for MEF2 expressed in muscle and brain reveals tissue-specific sequence constraints. J Biol Chem. 1995;270:23246–23249. doi:10.1074/jbc.270.40.23246.
3. Gossett LA, Kelvin DJ, Sternberg EA, Olson EN. A new myocyte-specific enhancer-binding factor that recognizes a conserved element associated with multiple muscle-specific genes. Mol Cell Biol. 1989;9:5022–5033. doi:10.1128/mcb.9.11.5022-5033.1989.
4. Kelly KK, Meadows SM, Cripps RM. Drosophila *Mef2* is an essential regulator of *Actin57B* transcription in cardiac, skeletal and visceral muscle lineages. Mech Dev. 2002;110:39–50. doi:10.1016/s0925-4773(01)00586-x.
5. Lin MH, Nguyen HT, Dybala C, Storti RV. Myocyte-specific enhancer factor 2 acts cooperatively with a muscle activator region to regulate Drosophila tropomyosin gene muscle expression. Proc Natl Acad Sci U S A. 1996;93:4623–4628. doi:10.1073/pnas.93.10.4623.
6. Sandmann T, Jensen LJ, Jakobsen JS, Karzynski MM, Eichenlaub MP, Bork P, Furlong EE. A temporal map of transcription factor activity: mef2 directly regulates target genes at all stages of muscle development. Dev Cell. 2006;10:797–807. doi:10.1016/j.devcel.2006.04.009.
7. Lin Q, Schwarz J, Bucana C, Olson EN. Control of mouse cardiac morphogenesis and myogenesis by transcription factor MEF2C. Science. 1997;276:1404–1407. doi:10.1126/science.276.5317.1404.
8. Potthoff MJ, Arnold MA, McAnally J, Richardson JA, Bassel-Duby R, Olson EN. Regulation of skeletal muscle sarcomeric integrity and postnatal muscle function by MEF2C. Mol Cell Biol. 2007;27:8143–8151. doi:10.1128/MCB.01187-07.
9. Naya FJ, Black BL, Wu H, Bassel-Duby R, Richardson JA, Hill JA, Olson EN. Mitochondrial deficiency and cardiac sudden death in mice lacking the MEF2A transcription factor. Nat Med. 2002;8:1303–1309. doi:10.1038/nm789.
10. Hinits Y, Hughes SM. Mef2s are required for think filament formation in nascent muscle fibers. Development. 2007;134:2511–2519. doi:10.1242/dev.007088.
11. Bour BA, O'Brien MA, Lockwood WL, Goldstein ES, Bodmer R, Taghert PH, Abmayr SM, Nguyen HT. Drosophila MEF2, a transcription factor that is essential for myogenesis. Genes Dev. 1995;9:730–741. doi:10.1101/gad.9.6.730.
12. Bryantsev AL, Baker PW, Lovato TL, Jaramillo MS, Cripps RM. Differential requirements for Myocyte enhancer factor-2 during adult myogenesis in Drosophila. Dev Biol. 2012;361:191–207. doi:10.1016/j.ydbio.2011.09.031.
13. Lilly B, Zhao B, Ranganayakulu G, Paterson BM, Schulz RA, Olson EN. Requirement of MADS domain transcription factor D-MEF2 for muscle formation in Drosophila. Science. 1995;267:688–693. doi:10.1126/science.7839146.
14. Soler C, Han J, Taylor MV. The conserved transcription factors Mef2 has multiple roles in adult Drosophila musculature formation. Development. 2012;139:1270–1275. doi:10.1242/dev.077875.

15. Black BL, Cripps RM. 2010 Myocyte enhancer factor-2 transcription factors in heart development and disease. In: Harvey RP and Rosenthal N, editors. Heart development and disease. New York: Academic Press.
16. Taylor MV. A novel Drosophila, mef2-regulated muscle gene isolated in a subtractive hybridisation-based molecular screen using small amounts of zygotic mutant RNA. Dev Biol. 2000;220:37–52. doi:10.1006/dbio.2000.9608.
17. Ranganayakulu G, Zhao B, Dokidis A, Molkentin JD, Olson EN, Schulz RA. A series of mutations in the D-MEF2 transcription factor reveal multiple functions in larval and adult myogenesis in Drosophila. Dev Biol. 1995;171:169–181. doi:10.1006/dbio.1995.1269.
18. Sparrow DB, Miska EA, Langley E, Reynaud-Deonauth S, Kotecha S, Towers N, Spohr G, Kouzarides T, Mohun TJ. MEF-2 function is modified by a novel co-repressor, MITR. embo J. 1999;18:5085–5098. doi:10.1093/emboj/18.18.5085.
19. Miska EA, Karlsson C, Langley E, Nielsen SJ, Pines J, Kouzarides T. HDAC4 deacetylase associates with and represses the MEF2 transcription factor. embo J. 1999;18:5099–5107. doi:10.1093/emboj/18.18.5099.
20. Lu J, McKinsey TA, Nicol RL, Olson EN. Signal-dependent activation of the MEF2 transcription factor by dissociation from histone deacetylases. Proc Natl Acad Sci U S A. 2000a;97:4070–4075. doi:10.1073/pnas.080064097.
21. Lu J, McKinsey TA, Zhang CL, Olson EN. Regulation of skeletal myogenesis by association of the MEF2 transcription factor with class II histone deacetylases. Mol Cell. 2000b;6:233–244. doi:10.1016/s1097-2765(00)00025-3.
22. Lemercier C, Verdel A, Galloo B, Curtet S, Brocard M-P, Khochbin S. mHDA1/HDAC5 histone deacetylase interacts with and represses MEF2A transcription factor. J Biol Chem. 2000;275:15594–15599. doi:10.1074/jbc.M908437199.
23. Molkentin JD, Li L, Olson EN. Phosphorylation of the MADS-box transcription factor MEF2C enhances its DNA binding ability. J Biol Chem. 1996;271:17199–17204. doi:10.1074/jbc.271.29.17199.
24. Han J, Jiang Y, Li Z, Kravchenko VV, Ulevitch RJ. Activation of the transcription factor MEF2C by the MAP kinase p38 in inflammation. Nature. 1997;386:296–299. doi:10.1038/386296a0.
25. Cox DM, Du M, Marback M, Yang ECC, Chan J, Siu KWM, McDermott JC. Phosphorylation motifs regulating the stability and function of Myocyte enhancer factor 2A. J Biol Chem. 2003;278:15927–15303.
26. Yang S-H, Galanis A, Sharrocks AD. Targeting of p38 mitogen-activated protein kinases to MEF2 transcription factors. Mol Cell Biol. 1999;19:4028–4038. doi:10.1128/MCB.19.6.4028.
27. Badodi S, Baruffaldi F, Ganassi M, Battini R, Molinari S. Phosphorylation-dependent degradation of MEF2C contributes to regulate G2/M transition. Cell Cycle. 2015;14:1517–1528. doi:10.1080/15384101.2015.1026519.
28. Di Giorgio E, Gagliostro E, Clocchiatti A, Brancolini C. The control operated by the cell cycle machinery on MEF2 stability contributes to the downregulation of CDKN1A and entry into S phase. Mol Cell Biol. 2015;35:1633–1647. doi:10.1128/MCB.01461-14.
29. Kyriakakis P, Tipping M, Abed L, Veraksa A. Tandem affinity purification in Drosophila. Fly. 2008;2:229–235. doi:10.4161/fly.6669.
30. Brand AH, Perrimon N. Targeted gene expression as a means of altering cell fates and generating dominant phenotypes. Development. 1993;118:401–415. doi:10.1242/dev.118.2.401.
31. Zaffran S, Astier M, Gratecos D, Semeriva M. The held out wings (how) Drosophila gene encodes a putative RNA-binding protein involved in the control of muscular and cardiac activity. Development. 1997;124:2087–2098. doi:10.1242/dev.124.10.2087.
32. Lovato TL, Benjamin AR, Cripps RM. Transcription of *Myocyte enhancer factor-2* in adult Drosophila myoblasts is induced by the steroid hormone ecdysone. Dev Biol. 2005;288:612–621. doi:10.1016/j.ydbio.2005.09.007.
33. Peckham M, Molloy JE, Sparrow JC, White DCS. Physiological properties of the dorsal longitudinal flight muscle and the tergal depressor of the trochanter muscle of Drosophila melanogaster. J Muscle Res Cell Motil. 1990;11:203–215. doi:10.1007/BF01843574.
34. Baker PW, Kelly Tanaka KK, Klitgord N, Cripps RM. Adult myogenesis in *Drosophila melanogaster* can proceed independently of Myocyte enhancer factor-2. Genetics. 2005;170:1747–1759. doi:10.1534/genetics.105.041749.
35. Lovato TL, Adams MM, Baker PW, Cripps RM. A molecular mechanism of temperature sensitivity for mutations affecting the Drosophila muscle regulator Myocyte enhancer factor 2. Genetics. 2009;183:107–117. doi:10.1534/genetics.109.105056.
36. Kocherlakota KS, Wu J-m, McDermott J, Abmayr SM. Analysis of the cell adhesion molecule Sticks-and-stones reveals multiple redundant functional domains, protein-interaction motifs and phosphorylated Tyrosines that direct myoblast fusion in Drosophila melanogaster. Genetics. 2008;178:1371–1383. doi:10.1534/genetics.107.083808.
37. Clark RI, Tan SWS, Pean CB, Roostalu U, Vivancos V, Bronda K, Pilatova M, Fu J, Walker DW, Berdeaux R, et al. MEF2 is an in vivo immune-metabolic switch. Cell. 2013;155:435–447. doi:10.1016/j.cell.2013.09.007.
38. Elgar SJ, Han J, Taylor MV. Mef2 activity levels differentially affect gene expression during Drosophila muscle development. Proc Natl Acad Sci U S A. 2008;105:918–923. doi:10.1073/pnas.0711255105.
39. Baruffaldi F, Montarras D, Basile V, De Feo L, Badodi S, Ganassi M, Battini R, Nicoletti C, Imbriano C, Musaro A, et al. Dynamic phosphorylation of the Myocyte enhancer factor 2Calpha1 splice variant promotes skeletal muscle regeneration and hypertrophy. Stem Cells. 2017;35:725–738. doi:10.1002/stem.2495.
40. Zhang CL, McKinsey TA, Olson EN. The transcriptional co-repressor MITR is a signal responsive inhibitor of myogenesis. Proc Natl Acad Sci U S A. 2001;98:7354–7359. doi:10.1073/pnas.131198498.
41. Sun L, Youn HD, Loh C, Stolow M, He W, Liu JO. Cabin 1, a negative regulator for calcieurin signaling in T-lymphocytes. Immunity. 1998;8:703–711. doi:10.1016/s1074-7613(00)80575-0.
42. Molkentin JD, Black BL, Martin JF, Olson EN. Cooperative activation of muscle gene expression by MEF2 and myogenic bHLH proteins. Cell. 1995;83:1125–1136. doi:10.1016/0092-8674(95)90139-6.
43. Kelly Tanaka KK, Bryantsev AL, Cripps RM. Myocyte enhancer factor-2 and Chorion factor-2 collaborate in activation of the myogenic program in Drosophila. Mol Cell Biol. 2008;28:1616–1629. doi:10.1128/MCB.01169-07.
44. Rubin GM, Spradling AC. Genetic transformation of Drosophila with transposable element vectors. Science. 1982;218:348–353. doi:10.1126/science.6289436.
45. Kane NS, Vora M, Varre KJ, Padgett RW. Efficient Screening of CRISPR/Cas9-Induced Events in Drosophila Using a Co-CRISPR Strategy. G3 GenesGenomesGenetics. 2017;7:87–93. doi:10.1534/g3.116.036723.
46. Vishal K, Lovato TL, Bragg C, Chechenova MB, Cripps RM. FGF signaling promotes myoblast proliferation through activation of Wingless signaling. Dev Biol. 2020;464:1–10. doi:10.1016/j.ydbio.2020.05.009.
47. Morriss GR, Bryantsev AL, Chechenova M, LaBeau EM, Lovato TL, Ryan KM and Cripps RM. Analysis of skeletal muscle development in Drosophila. In: DiMario J, editors. Myogenesis: methods and protocols. New York: Springer; 2011.
48. Drummond DR, Hennessey ES, Sparrow JC. Characterisation of missense mutations in the Act88F gene of *Drosophila melanogaster*. Mol Gen Genet. 1991;226:70–80. doi:10.1007/BF00273589.